Electron beam-induced absorption modulation imaging of strained $In_{0.2}Ga_{0.8}As/GaAs$ multiple quantum wells

D. H. Rich, K. Rammohan, Y. Tang, and H. T. Lin
Photonic Materials and Devices Laboratory, Department of Materials Science and Engineering, University of Southern California, Los Angeles, California 90089-0241

J. Maserjian and F. J. Grunthaner
Center for Space Microelectronics Technology, Jet Propulsion Laboratory, California Institute of Technology, Pasadena, California 91109

A. Larsson
Chalmers University of Technology, Department of Optoelectronics, and Electrical Measurements, S-412 96 Göteborg, Sweden

S. I. Borenstain
Jerusalem College of Technology, Jerusalem, Israel 91160

(Received 27 January 1993; accepted for publication 22 April 1993)

We have examined the effects of electron-hole plasma generation on excitonic absorption phenomena in *nipi*-doped $In_{0.2}Ga_{0.8}As/GaAs$ multiple quantum wells (MQWs) using a novel technique called electron beam-induced absorption modulation imaging. The electron-hole plasma is generated by a high-energy electron beam in a scanning electron microscope and is used as a probe to study the MQW absorption modulation. The influence of structural defects on the diffusive transport of carriers is imaged with a μm-scale resolution.

Periodic *nipi* doping of multiple quantum well (MQW) structures allows for the formation of a spatially separated electron-hole plasma, which can be excited by relatively weak external light or electron beams due to the large enhancement in the excess carrier lifetime.[1–6] These structures exhibit large photo-optic effects which can be utilized for applications in *all-optical* spatial light modulators (SLMs) which are the building blocks of high-information throughput optical computing elements and Fourier-plane image processing devices.[2–5] The InGaAs/GaAs MQW system, owing largely to the transparent nature of the GaAs substrate with respect to the MQW interband transition energies, is a leading candidate for the fabrication of SLMs.[3–6] We demonstrate in this letter that the spatially separated electron-hole plasma can be used as a probe to study the electronic and structural properties of defects which can exist in the MQW regions with a μm-scale spatial resolution. The present results demonstrate that in certain *lattice-mismatched* heterostructures, a Cottrell atmosphere of point defects that is well separated from interface misfit dislocation cores can affect excess carrier lifetimes and the lateral transport of carriers.

Using a novel technique called electron beam-induced absorption modulation imaging (EBIA), we examine the influence of defects on the ambipolar diffusive transport in *nipi*-doped $In_{0.2}Ga_{0.8}As/GaAs$ MQWs. In EBIA, the excess carriers are generated by a high-energy electron beam within a scanning electron microscope (SEM).

The experimental setup utilizes a modified cathodoluminescence (CL) system to collect light which is transmitted through the MQW structure as illustrated in Fig. 1(a). A multimode optical fiber with a 100 μm core diameter is used to transmit light from a tungsten light source dispersed by a monochromator to the backside of the sample in the SEM vacuum chamber. The technique utilizes lock-in detection by chopping the light source from the monochromator or by blanking the electron beam source. The images reveal an absorption modulation contrast caused by the influence of intrinsic and extrinsic recombination channels on the diffusion of spatially separated carriers to the vicinity of the optical fiber.

The sample (designated D92) was grown by molecular beam epitaxy, and consists of 44 $In_{0.2}Ga_{0.8}As$ QWs, each 65 Å wide, and separated by 780 Å thick GaAs barriers. In the center of each GaAs barrier a *p*-type Be-doping plane with a sheet density of 9.0×10^{12} cm^{-2} was inserted. On both sides of the QWs, using 100 Å thick spacer layers, *n*-type Si-doping planes with a sheet density of 3.0×10^{12} cm^{-2} were inserted. The δ doping causes a linear variation in the band edges along the growth direction, as shown in Fig. 1(b). During electron-hole pair generation, electrons will be attracted to the QWs and the holes to the barrier region midway between the wells, resulting in their spatial separation. The recombination of the spatially separated carriers occurs through spatially indirect radiative tunneling recombination and spatially direct recombination of thermally excited carriers, as denoted schematically by the lifetimes τ_I and τ_D, respectively, in Fig. 1(b).

Absorption spectra (solid lines) for various electron beam currents, I_b, are shown in Fig. 2 at a sample temperature of 115 K, and were obtained by chopping the monochromator probe. The effective QW absorption coefficients were calculated according to $(-L_{\mathrm{eff}})^{-1}\ln T$, where T is the measured normalized transmission through the sample and L_{eff} is the total thickness of the MQW structure. The total light power through the fiber was $\sim10^{-7}$ W with a spectral resolution of 1 nm. The hh1-e1 exciton peak, which is located at $\lambda=948$ nm, is seen to quench as the current level is increased; this is a result of the screening of the Coulomb interaction in the QWs by the electron

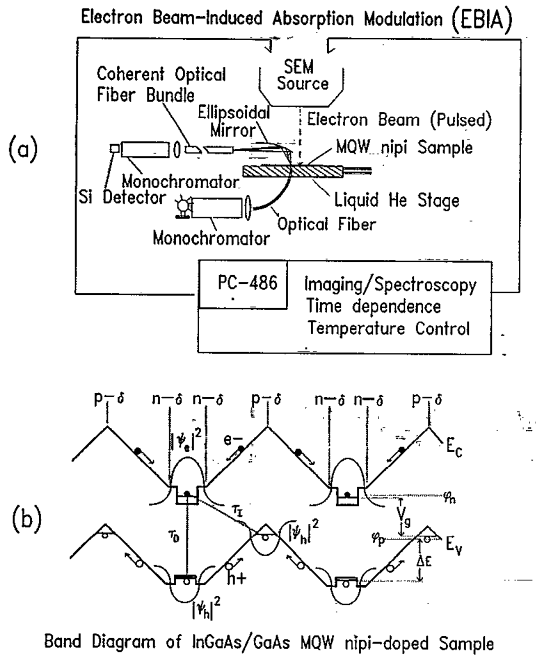

FIG. 1. Schematic of electron beam-induced absorption modulation imaging and cathodoluminescence setup in (a). Band diagram of a MQW *nipi* structure showing spatial separation of electrons and holes which occurs under electron beam excitation (b). The structure is illustrated for the case of δ doping, which results in linear variations in the conduction (E_C) and valence (E_V) band edges relative to the quasi Fermi levels for electrons and holes (ϕ_n and ϕ_p, respectively).

plasma.[2] The differential absorption spectrum (dashed curve of Fig. 2) was obtained by chopping the electron beam, this enables an observation of the higher lying excitonic transitions. The quenching of the hh1-e1 exciton absorption coefficient in Fig. 2 is seen to depend approximately logarithmically on the beam current as expected from the reduction of the recombination lifetime with increasing carrier density.[2,3]

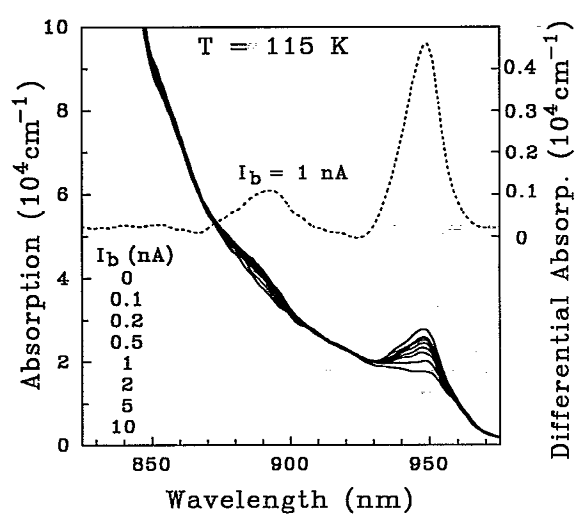

FIG. 2. EBIA spectroscopy measurement of a *nipi*-doped MQW sample for room temperature. Differential EBIA spectroscopy measurements (dashed lines) are obtained by blanking the electron beam source.

A panchromatic CL image of the sample is shown in Fig. 3(a) with a 115 K temperature. The CL luminescence is primarily due to the MQW exciton associated with the e1-hh1 transition.[7,8] The dark line defects (DLDs) are oriented along the [1$\bar{1}$0] and [110] directions, and they are a result of strain-induced interface misfit dislocations. Based on previous CL and transmission electron microscopy data, Rich and co-workers have proposed that a Cottrell atmosphere of point defects in the MQW region is responsible for the *nonradiative* recombination associated with the DLDs.[7,8] It is possible to obtain spatial information concerning changes in the differential absorption by scanning the electron beam within the vicinity of the optical fiber center. An EBIA image [shown in Fig. 3(b) for $T=115$ K], was obtained by detecting the transmitted signal at $\lambda=948$ nm, corresponding to the e1-hh1 exciton absorption. The electron beam ($I_b=1$ nA) was pulsed at a fixed frequency of 500 Hz while rastered in two dimensions across the sample to generate a 640$\times$480 pixel image with the differential absorption intensity value stored in 1 byte of memory per pixel. The EBIA image of Fig. 3(b) shows the influence of structural defects on the diffusive transport of carriers with a μm-scale resolution. The center of the bright spot in Fig. 3(b) corresponds to the region of greatest excess carrier density and the region where the electron beam causes the largest transmission modulation, which is near the center of the optical fiber. A histogram of the imaging results of Fig. 3 is presented in Fig. 4. The curves illustrate the intensity versus electron beam position relative to the fiber center (distance=0) along the [110]-oriented line shown in Fig. 3(b) for CL, the absorption modulation $\Delta\alpha$, and its derivative $\partial\Delta\alpha/\partial x$. The center of the steps in $\Delta\alpha$ show up as peaks in the derivative scan. Vertical dotted lines are drawn in the figure to illustrate the strong correlation between dips and shoulders in the CL intensity at DLDs and the positions of the steps observed in the absorption modulation. These results demonstrate, remarkably, that the orientation and positions of steps seen in the absorption modulation correspond with the orientation and position of DLDs seen in the CL image. The transport of electrons and holes is, therefore, influenced by the presence of a Cottrell atmosphere of point defects which is well separated spatially from the interface misfit dislocations.[8]

The presence of point defects lying in the regions delineated by the DLDs in CL imaging can influence the diffusion process in the following ways: (i) by creating diffusion barriers, (ii) by creating midgap recombination centers, and (iii) by affecting the lifetime of spatially indirect transitions. Point defects can create local variations in the band edges relative to the Fermi level; the depletion length will depend on the charge associated with the defect and the local dopant concentration. Since the electrons and holes in the plasma are confined to the *n*- and *p*-type regions, respectively [see Fig. 1(b)], a defect-induced change in the band edges will push the Fermi level (or quasi-Fermi level under excitation) closer to the middle of the gap. In case (i), this bandbending will cause the majority carriers to be repelled from the point defects and the Cottrell at-

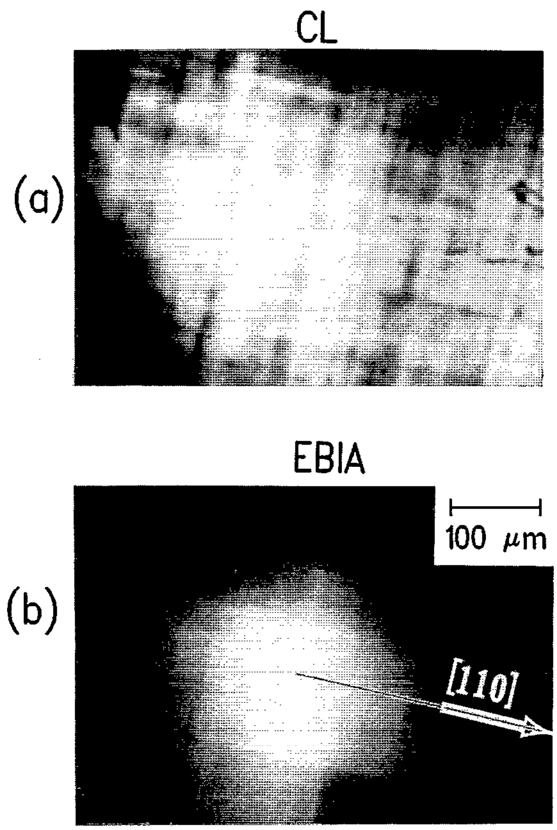

FIG. 3. Cathodoluminescence image (a) and EBIA image (b) of the same region of a *nipi*-doped MQW structure. The CL image of the e-hh exciton luminescence is represented by a gray scale, where bright regions correspond to an increase in luminescence intensity relative to darker regions. DLDs are observed to run along both [110] directions. The EBIA image is displayed using a gray scale for the absorption modulation intensity. DLDs are seen to correspond with the positions and orientations of absorption modulation steps, which are represented by sharp changes in intensity along the same high symmetry [110] directions in (b).

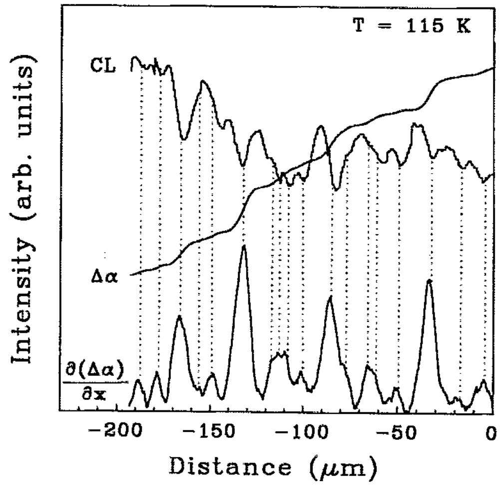

FIG. 4. Histograms (intensity vs position) of CL, absorption modulation ($\Delta\alpha$), and its derivative $\partial\Delta\alpha/\partial x$ as a function of the distance (x) from the center of the optical fiber along [110]. The center of the steps in the absorption modulation (peaks in the derivative) are seen to correlate strongly with the minima and shoulders seen in the CL line scan. The minima in the CL scans correspond to the dark line defects seen in the CL image of Fig. 3(a).

mosphere of defects will act as a barrier to diffusion.[9] A large excess carrier concentration will reduce the band bending, in a manner similar to the barrier reduction which occurs in a surface photovoltaic shift. In case (ii), the barrier reduction will result in an attendant increase in overlap between wave functions of the midgap defect states and the majority carriers. Also, thermally assisted defect-induced recombination of majority carriers can occur at high temperatures. This is similar to the existence of thermal activation barriers for minority carriers caused by defects in uniformly doped semiconductors which causes the enhancement of nonradiative recombination at high temperatures.[10] In case (iii), a large density of point defects will increase the average value of the effective band gap V_g [reduce the barrier height ΔE in Fig. 1(b)], resulting in a smaller value of τ_l. While the three cases are not exhaustive, they illustrate possible ways in which a Cottrell atmosphere of defects can cause the measured steplike response in the EBIA image of Fig. 3(b).

Recent theoretical calculations by Jonsson *et al.* have shown that the lifetime for an ideal $In_{0.2}Ga_{0.8}As$/GaAs MQW *nipi*-doped structure is several orders of magnitude longer than the lifetime measured by an optically induced absorption modulation technique.[11] The primary cause suggested for this lifetime discrepancy was a spatial redistribution of dopants which would lead to an effective decrease in ΔE, and thus increase in tunneling recombination and spatially direct recombination of thermally excited carriers.[11] The present structure in the EBIA imaging results demonstrate that extrinsic defect related mechanisms can also affect the absorption modulation, excess carrier lifetime and carrier transport.

This work was supported by grants from the USC James H. Zumberge Faculty Research and Innovation Fund and the Charles Lee Powell Foundation.

[1] G. H. Döhler, IEEE J. Quantum Electron. **22**, 1682 (1986); J. Vac. Sci. Technol. B **1**, 278 (1983).
[2] J. Maserjian, P. O. Andersson, B. R. Hancock, J. M. Iannelli, S. T. Eng, F. J. Grunthaner, K.-K. Law, P. O. Holtz, R. J. Simes, L. A. Coldren, A. C. Gossard, and J. L. Merz, Appl. Opt. **28**, 4801 (1989).
[3] A. Larsson and J. Maserjian, Appl. Phys. Lett. **58**, 1946 (1991); A. Larsson and J. Maserjian, Opt. Eng. **31**, 1576 (1992).
[4] A. Larsson and J. Maserjian, Appl. Phys. Lett. **59**, 3099 (1991).
[5] N. Streibl, K.-H. Brenner, A. Huang, J. Jahns, J. Jewell, A. W. Lohmann, D. A. B. Miller, M. Murdocca, M. E. Prise, and T. Sizer, Proc. IEEE **77**, 1954 (1989).
[6] J. M. Iannelli, J. Maserjian, B. R. Hancock, P. O. Andersson, and F. J. Grunthaner, Appl. Phys. Lett. **54**, 301 (1989).
[7] D. H. Rich, K. C. Rajkumar, Li Chen, A. Madhukar, T. George, J. Maserjian, F. J. Grunthaner, and A. Larsson, J. Vac. Sci. Technol. B **10**, 1965 (1992).
[8] D. H. Rich, T. George, W. T. Pike, J. Maserjian, F. J. Grunthaner, and A. Larsson, J. Appl. Phys. **72**, 5834 (1992).
[9] The resulting localized bandbending in the vicinity of defects will repel the majority carrier plasma in a manner similar to the repulsion and attraction of majority and minority carriers, respectively, at semiconductor surfaces.
[10] See, e.g., J. I. Pankove, *Optical Processes in Semiconductors* (Dover, New York, 1971), pp. 165–166.
[11] B. Jonsson, A. G. Larsson, O. Sjölund, S. Wang, T. Andersson, and J. Maserjian (unpublished).